Magnetic Trapping of Long-Lived Cold Rydberg Atoms

J.-H. Choi, J. R. Guest,* A. P. Povilus, E. Hansis,† and G. Raithel
FOCUS Center, Department of Physics, University of Michigan, Ann Arbor, Michigan 48109-1040, USA
(Received 9 August 2005; published 5 December 2005)

We report on the trapping of long-lived strongly magnetized Rydberg atoms. ^{85}Rb atoms are laser cooled and collected in a superconducting magnetic trap with a strong bias field (2.9 T) and laser excited to Rydberg states. Collisions scatter a small fraction of the Rydberg atoms into long-lived high-angular momentum ''guiding-center'' Rydberg states, which are magnetically trapped. The Rydberg atomic cloud is examined using a time-delayed, position-sensitive probe. We observe magnetic trapping of these Rydberg atoms for times up to 200 ms. Oscillations of the Rydberg-atom cloud in the trap reveal an average magnetic moment of the trapped Rydberg atoms of $\approx -8\mu_B$. These results provide guidance for other Rydberg-atom trapping schemes and illuminate a possible route for trapping antihydrogen.

DOI: 10.1103/PhysRevLett.95.243001 PACS numbers: 32.60.+i, 32.10.Dk, 32.80.Pj, 32.80.Rm

Laser cooling and trapping methods have been used to study atoms, ions, molecules, and plasmas, leading to an unprecedented level of control for the systems [1–4]. The ability to trap cold atoms in highly excited Rydberg states [5], as has been proposed by a number of authors [6–8], may also open new avenues in a variety of fields, including quantum information processing [9–12] and coherent control of Rydberg interactions in cavity-QED experiments [7,13,14]. In antihydrogen research [15,16], trapping of the recombined antihydrogen Rydberg atoms [17] during their decay into lower-lying states will be crucial for collecting antiatoms for fundamental symmetry tests. Rydberg-atom traps could also be used to study collective effects in cold Rydberg gases [18,19] and perform precision measurements [6].

In this Letter, we report on the trapping of long-lived high-angular momentum Rydberg atoms of ^{85}Rb in a superconducting magnetic atom trap with a strong bias magnetic field of 2.9 T [20]. In a classical picture, the Rydberg electron in these atoms [21,22] follows characteristic $\mathbf{E} \times \mathbf{B}$ drift orbits which resemble charged particle orbits in Penning traps [Fig. 1(a)]. These guiding-center drift atoms, presumably observed in recent antihydrogen experiments [17], are characterized by large and negative values of the magnetic quantum number ($|m| > 100$), and are expected to live for hundreds of ms [23]. To produce drift atoms, we first laser excite low-$|m|$ Rydberg atoms. In the following tens of μs, these atoms undergo collisions with free electrons and presumably with other Rydberg atoms [24,25]. These collisions involve transient transverse electric fields which can cause m mixing and thereby partially transform the population into high-$|m|$ drift Rydberg states. The free electrons may be generated through Penning-ionizing collisions between Rydberg atoms, which have been observed to generate free electrons with energies in the range of 10 meV at low magnetic field [26]. Indeed, these collisions may be favored in strong magnetic fields due to the large permanent electric quadrupole moments which characterize strongly magnetized Rydberg atoms. Free electrons may also be generated by photoionization of a small fraction of trapped atoms by spurious ionizing radiation in the laser pulse (amplified spontaneous emission). Experimental evidence suggests that, under typical conditions in our trap, $\sim 1\%$ of the initially excited Rydberg atoms evolve into high-$|m|$ drift states. The details of this evolution will be further investigated.

The magnetic trapping of high-$|m|$ Rydberg atoms in a strong, nonuniform magnetic field $\mathbf{B}$ can be understood by examining the magnetic-dipole potential experienced by the Rydberg electron [Fig. 1(b)]. Since the internal atomic Coulomb forces ($\mathbf{F}_{\mathrm{Coul}}$) cancel, the magnetic force on the Rydberg electron ($\mathbf{F}_{\mathrm{B}}$) equals the net trapping force on the entire Rydberg atom. Neglecting the magnetic moment due to the magnetron motion of the Rydberg electron, the quantum-mechanical trapping potential $V_{\mathrm{R}}(\mathbf{r})$ for drift

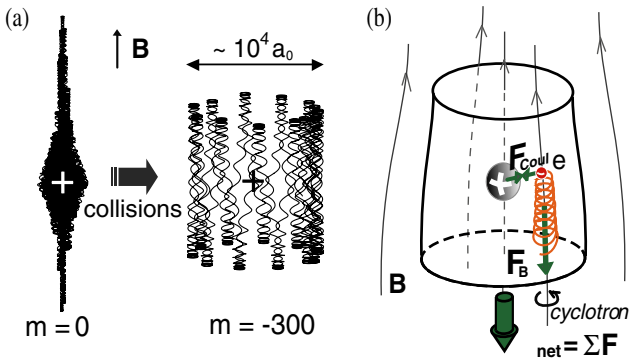

FIG. 1 (color online). (a) Collisions transform laser excited low-$|m|$ Rydberg atoms into drift-state Rydberg atoms. The associated dramatic change in the nature of the atoms is qualitatively visualized by depicting classical Rydberg electron trajectories for $m = 0$ and $m = -300$ (a_0: Bohr radius). Strongly magnetized atoms have permanent electric quadrupole moments. (b) Force diagram in a drift Rydberg atom. The Rydberg electron moves in a Penning-trap-like orbit on a cylindrical surface. In an inhomogeneous magnetic field, a magnetic-bottle force $\mathbf{F}_{\mathrm{B}}$ is acting on the electron's cyclotron orbit. Since the internal atomic Coulomb forces $\mathbf{F}_{\mathrm{Coul}}$ cancel, the net trapping force $\mathbf{F}_{\mathrm{net}}$ is equivalent to the average magnetic-bottle force $\mathbf{F}_{\mathrm{B}}$.

Rydberg atoms equals the free-electron potential, which is, in atomic units [27],

$$V_R(\mathbf{r}) = (n_c + m_s + 1/2)|\mathbf{B}(\mathbf{r})| = -\mu_{\text{eff}}|\mathbf{B}(\mathbf{r})|. \quad (1)$$

Here, n_c and m_s are the cyclotron and electron spin quantum numbers, respectively, and μ_{eff} denotes the component of the effective magnetic moment of the Rydberg atom parallel to $\mathbf{B}$. The trapping potential does not depend on m because drift Rydberg atoms have negative m, as explained in Ref. [23]. In classical electrodynamics, $V_R(\mathbf{r})$ is equivalent to the potential that is responsible for magnetic-bottle forces on charged particles parallel to B-field lines [28]. Note that in Eq. (1), μ_{eff} is always negative, implying that all atoms would be low-field seeking and could therefore be magnetically trapped.

However, if we consider the Rydberg electron's magnetron motion, we find a mitigating positive contribution to μ_{eff} due to the antiparallel nature of the magnetron and cyclotron magnetic moments. For example, consider the special case of planar motion of the Rydberg electron in the plane transverse to $\mathbf{B}$. In this case, the $\mathbf{E} \times \mathbf{B}$-drift velocity of the Rydberg electron and the area of the circular magnetron orbit yield a magnetron magnetic moment of $+\frac{1}{B\rho_e}$, where the radius of the magnetron orbit, ρ_e, is related to the magnetic quantum number via $m = -\frac{1}{B\rho_e^3} - \frac{1}{2}B\rho_e^2$. Thus, for planar drift states the magnetic moment is

$$\mu_{\text{eff}} = -(n_c + m_s + 1/2) + \frac{1}{B\rho_e}. \quad (2)$$

The positive correction term caused by the magnetron motion obviously reduces the magnetic-trapping force and, for sufficiently small ρ_e, reverses the sign of μ_{eff}. Therefore, due to the magnetron motion not all drift Rydberg states are magnetically trapped.

In the experiment, cold Rydberg atoms are generated through two-stage laser excitation on a 5 Hz cycle. ^{85}Rb atoms are first laser cooled to the Doppler temperature ($\approx$140 μK) and magnetically trapped at 2.9 T in a superconducting Ioffe-Pritchard trap [20]. After laser excitation from the $5S$ (ground) to the $5P$ state, the atoms are further excited by a pulsed dye laser (10 ns duration, 3 mJ/pulse) to a Rydberg state with an energy 6.5 cm^{-1} below the ionization threshold. In the B-field-free case, this binding energy would correspond to a principal quantum number $n \approx 130$ and to atomic diameters of ≈ 2 μm. On a time scale of tens of μs, the laser excited Rydberg atoms undergo m-mixing collisions [29] and partially evolve into drift states. At a variable time t after the laser excitation, Rydberg atoms in the trap region are imaged and counted with background-free field ionization (FI). By applying an electric field ramp to the Rydberg atoms, the weakly bound electrons are stripped from their parent atoms and guided down the B-field lines onto a double micro-channel plate and phosphor screen located 47 cm from the trap center. The strong B field provides high collection efficiency and maintains the spatial information of the Rydberg cloud because the electrons remain pinned to the B-field lines passing through the parent atoms. Because of details in the magnetic field topology, the circular cross section of the atom cloud is mapped onto an elliptical area with an aspect ratio of 23:1.

Spatially resolved images of the Rydberg-atom clouds for FI-delay times up to 110 ms are shown in Fig. 2. The result indicates both the formation and the trapping of drift Rydberg atoms. First, atoms detected after 10 ms are predominantly in drift states because laser excited low-$|m|$ Rydberg atoms have much shorter radiative decay times. Second, the spatial distribution of Rydberg atoms at times up to 110 ms is not significantly different from that after 10 ms, suggesting that the atoms are trapped. Note that in 110 ms the center of mass of a free-falling atom cloud would have dropped 6 cm, equivalent to 3 times the vertical range of view corresponding to the phosphor screen's diameter.

The decay of the population of trapped Rydberg atoms is further investigated in Fig. 3 (filled circles). Rydberg atoms are detected in the trap region at times up to 200 ms after the initial excitation. One out of 10^5 laser excited low-$|m|$ Rydberg atoms survives for 200 ms. The lifetime extracted from the decay curve increases from $\approx$ 10 ms for detection times less than 80 ms to $\approx$ 80 ms thereafter. We believe that most of the decay is due to radiative transitions into lower-lying states that cannot be detected or into high-field-seeking states that are expelled from the trap. Because of the low radiation temperature (4 K) and the low densities of trapped drift Rydberg atoms, decay of the Rydberg atoms due to thermal ionization or ionizing Rydberg-Rydberg collisions is unlikely.

To verify magnetic confinement, we have performed a reference measurement with the transverse confinement coils turned off. In this mode of operation, the field amplitude has a saddle point at the trap center (Fig. 3, inset for

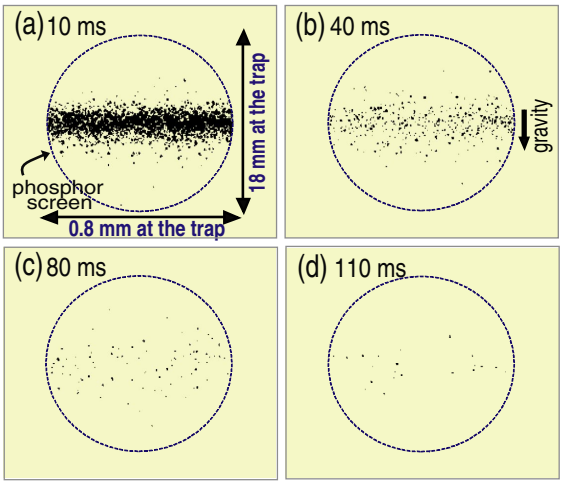

FIG. 2 (color online). (a)–(d) Phosphor images of electrons from field ionization at different times of Rydberg-atom detection. Each dot represents a field-ionized Rydberg atom. The decrease in the Rydberg counts is discussed in the text.

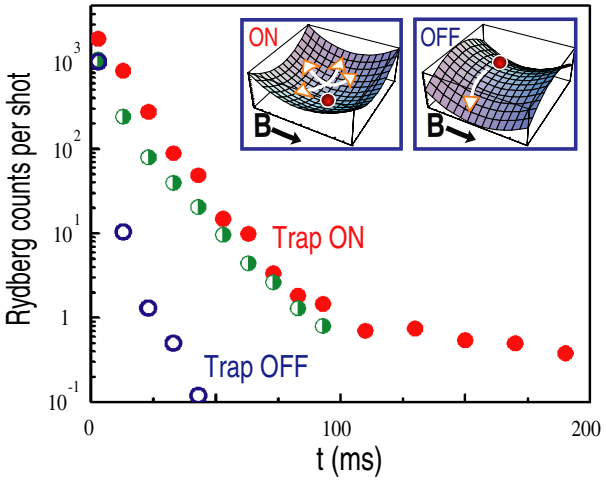

FIG. 3 (color online). Rydberg-atom counts vs time of Rydberg-atom detection, averaged over 500 cycles. Trap ON: Measurement results for a typical trapping configuration. Filled circles: initial Rydberg-atom number 10^5 and density 10^7 cm^{-3}. Half-filled circles: initial Rydberg-atom number 10^4 and density 10^6 cm^{-3}. Trap OFF, open circles: Measurement result with the transverse confinement coils turned off and with an initial Rydberg-atom number 10^5 and density 10^6 cm^{-3}. The systematic background count is less than 0.02 per shot. Insets: The B-field magnitude has a minimum at the center location in the trap-on case, while it has a saddle point in the trap-off case.

trap-off case), and atoms are expelled from the trap region in the directions transverse to the B field. As expected, without the transverse confinement the measured Rydberg counts (open circles) reveal a significantly faster decrease of the population. The number of Rydberg atoms detected at 40 ms delay is a factor of 400 less than the number detected with the trap enabled.

Without the transverse confinement, the initial density of Rydberg atoms that can be achieved is reduced by about a factor of 10 with respect to the trap-on case. Therefore, one may suspect that the difference between the trap-on case (filled circles) and the trap-off case (open circles) of Fig. 3 mostly lies in the lack of collisions that promote Rydberg atoms from their initial state into the long-lived drift states. In order to exclude this possibility, we have performed a trap-on measurement in which the initial density of Rydberg atoms has been reduced to a value equivalent to that of the trap-off case. The result (half-filled circles in Fig. 3) affirms that it is indeed the magnetic confinement, not the density, which is responsible for the long dwell times of the Rydberg atoms in the detection region, observed in the trap-on case.

Considering Eqs. (1) and (2) and noting that the ground-state magnetic moment is, in our case, $\mu_G = -\frac{1}{2}$, the average trapping force becomes stronger by a factor $2\mu_{\text{eff}}$ as ground-state atoms are excited and evolve into magnetically trapped drift Rydberg states. Because of the sudden change in trap depth, spatial oscillations of Rydberg clouds are expected [Fig. 4(a)]. With the known value of the oscillation period of the ground-state atom trap (52 ms), the measured oscillation period of the Rydberg cloud provides information on the average value of μ_{eff}.

The center-of-mass position of the ground-state atom cloud can be adjusted by varying the detailed radiation-pressure conditions in the atom trap. In Fig. 4(c), the initial cloud position is close to its equilibrium position, leading to a Rydberg-atom cloud evolution that is strongly dominated by a breathing-mode oscillation. A modulation in the size of the atom cloud is observed as the Rydberg-atom detection time is varied. In Fig. 4(e), the standard deviation of the distributions measured in Fig. 4(c) is plotted vs the detection time (circles). The breathing-mode oscillation period is determined to be ≈ 9 ms. Considering that the breathing frequency equals twice the fundamental oscilla-

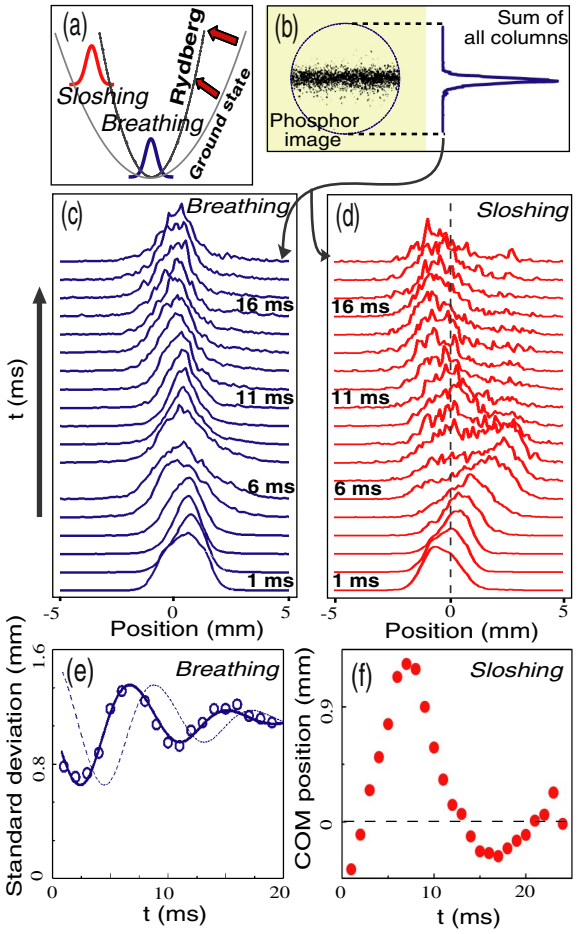

FIG. 4 (color online). (a) An increase in the trap depth can cause two types of oscillatory motion of the Rydberg-atom cloud. (b) The vertical profile of the cloud is obtained by integrating the phosphor screen images along the horizontal direction. One-dimensional vertical profiles of the clouds at different Rydberg-atom detection times show (c) breathing and (d) sloshing motions of the Rydberg-atom cloud. (e) Circles: standard deviations of the distributions in (c) vs Rydberg-atom detection time. Lines: simulation results (explained in the text). (f) Average positions of the distributions in (d) vs detection time.

tion frequency, it is concluded that $\bar{\mu}_{\rm eff} \approx -4.0$ (overbar represents an ensemble average), indicating an order of magnitude increase in trap depth in comparison with ground-state atom trapping ($\mu_{\rm G} = -1/2$).

The breathing-mode oscillation in Fig. 4(e) displays a pronounced decay of the oscillation amplitude. This is attributed to the fact that different atoms, with different $\mu_{\rm eff}$, oscillate at different frequencies, leading to inhomogeneous dephasing and to a decay of the net oscillation signal. To obtain an estimate for the width of the $\mu_{\rm eff}$ distribution, we have fit the data assuming Gaussian probability distributions of $\mu_{\rm eff}$ with an average $\bar{\mu}_{\rm eff} = -4.0$ and a variable width. We have found best agreement for a standard deviation $\Delta\mu_{\rm eff} = 1.4$ (dotted line). The agreement between experimental data and simulation is improved considerably by shifting the fitted result by -2 ms (solid line). We believe that this phase shift is due to transient forces acting on the Rydberg atoms during the initial stages of their evolution from low $|m|$ into drift states.

A sloshing motion of the Rydberg-atom cloud can be induced by initially creating the Rydberg-atom cloud with a displacement from the equilibrium position [Figs. 4(d) and 4(f)]. As expected, the oscillation period of the sloshing motion of the average cloud position is found to be ≈ 18 ms, i.e., twice the period of the breathing oscillation.

Rydberg atoms in strong magnetic fields have several properties which we believe have been beneficial in realizing a robust trap. We have found in calculations that the majority of drift Rydberg atoms produced are attracted to the minimum of the B field, regardless of their internal states, and are therefore suitable for magnetic trapping. As a result, state-changing collisions and radiative interactions are quite unlikely to turn a magnetically trapped Rydberg atom into an untrapped one. Further, Rydberg atoms in strong magnetic fields are nondegenerate and have no permanent electric dipole moments, and, consequently, their susceptibility to electric fields is lower than that of most Rydberg states in weak fields. Therefore, strong-magnetic-field Rydberg-atom traps are less likely to be compromised by stray electric fields than low-magnetic-field ones.

In summary, we have demonstrated the magnetic trapping of drift Rydberg atoms produced by Rydberg-atom collisions. The observation of oscillatory motion of Rydberg atoms in the magnetic potential has provided the most compelling evidence that long-lived Rydberg atoms have been trapped. A common principle of all Rydberg-atom trapping methods is that, due to the quasifree nature of the Rydberg electron, the Rydberg energy levels can be easily varied in a controlled manner by inhomogeneous external fields. We believe that this general quality of Rydberg atoms will be important in other Rydberg-atom trapping methods that might emerge in the future.

The authors would like to thank P. H. Bucksbaum for the generous loaning of equipment. We also thank D. G. Steel for helpful discussions. This work was supported by the Chemical Sciences, Geosciences and Biosciences Division of the Office of Basic Energy Sciences, Office of Science, U.S. Department of Energy.

*Present address: Physics Division, Argonne National Laboratory, Argonne, IL 60439, USA.
†Present address: Max-Planck-Institut für Quantenoptik, Hans-Kopfermann-Straße 1, 85748 Garching, Germany.

[1] H. J. Metcalf and P. van der Straten, *Laser Cooling and Trapping* (Springer-Verlag, New York, 1999).
[2] C. E. Wieman, D. E. Pritchard, and D. J. Wineland, Rev. Mod. Phys. **71**, S253 (1999).
[3] J. D. Weinstein, R. deCarvalho, T. Guillet, B. Friedlich, and J. M. Doyle, Nature (London) **431**, 281 (2004).
[4] T. C. Killian *et al.*, Phys. Rev. Lett. **83**, 4776 (1999).
[5] T. F. Gallagher, *Rydberg Atoms* (Cambridge University Press, New York, 1994).
[6] S. K. Dutta, J. R. Guest, D. Feldbaum, A. Walz-Flannigan, and G. Raithel, Phys. Rev. Lett. **85**, 5551 (2000).
[7] P. Hyafil *et al.*, Phys. Rev. Lett. **93**, 103001 (2004).
[8] I. Lesanøvsky and P. Schmelcher, Phys. Rev. Lett. **95**, 053001 (2005).
[9] J. M. Raimond, M. Brune, and S. Haroche, Rev. Mod. Phys. **73**, 565 (2001).
[10] D. Jaksch *et al.*, Phys. Rev. Lett. **85**, 2208 (2000).
[11] M. D. Lukin *et al.*, Phys. Rev. Lett. **87**, 037901 (2001).
[12] A. S. Sorensen, C. H. van der Wal, L. I. Childress, and M. D. Lukin, Phys. Rev. Lett. **92**, 063601 (2004).
[13] S.-B. Zheng and G.-C. Guo, Phys. Rev. Lett. **85**, 2392 (2000).
[14] S. Osnaghi *et al.*, Phys. Rev. Lett. **87**, 037902 (2001).
[15] M. Amoretti *et al.*, Nature (London) **419**, 456 (2002).
[16] G. Gabrielse *et al.*, Phys. Rev. Lett. **89**, 213401 (2002).
[17] G. Gabrielse *et al.*, Phys. Rev. Lett. **89**, 233401 (2002).
[18] R. Côte, Phys. Rev. Lett. **85**, 5316 (2000).
[19] F. Robicheaux, J. V. Hernández, T. Topçu, and L. D. Noordam, Phys. Rev. A **70**, 042703 (2004).
[20] J. R. Guest, J.-H. Choi, E. Hansis, A. P. Povilus, and G. Raithel, Phys. Rev. Lett. **94**, 073003 (2005).
[21] M. E. Glinsky and T. M. O'Neil, Phys. Fluids B **3**, 1279 (1991).
[22] J. R. Guest and G. Raithel, Phys. Rev. A **68**, 052502 (2003).
[23] J. R. Guest, J.-H. Choi, and G. Raithel, Phys. Rev. A **68**, 022509 (2003).
[24] S. K. Dutta, D. Feldbaum, A. Walz-Flannigan, J. R. Guest, and G. Raithel, Phys. Rev. Lett. **86**, 3993 (2001).
[25] A. Walz-Flannigan, J. R. Guest, J.-H. Choi, and G. Raithel, Phys. Rev. A **69**, 063405 (2004); W. Li *et al.*, Phys. Rev. A **70**, 042713 (2004).
[26] W. Li, P. J. Tanner, and T. F. Gallagher, Phys. Rev. Lett. **94**, 173001 (2005).
[27] L. D. Landau and E. M. Lifshitz, *Quantum Mechanics: Non-Relativistic Theory* (Pergamon Press, New York, 1977), 3rd ed.
[28] J. D. Jackson, *Classical Electrodynamics* (John Wiley & Sons, New York, 1999), 3rd ed.
[29] J. H. Choi, J. R. Guest, E. Hansis, A. P. Povilus, and G. Raithel, Phys. Rev. Lett. (to be published).